



HAL
open science

A detailed paleomagnetic record between 2.1 and 2.75 Ma at IODP Site U1314 in the North Atlantic: Geomagnetic excursions and the Gauss-Matuyama transition

Masao Ohno, Tatsuya Hayashi, Fumiki Komatsu, Fumi Murakami, Meng Zhao, Yohan Guyodo, Gary Acton, Helen F. Evans, Toshiya Kanamatsu

► To cite this version:

Masao Ohno, Tatsuya Hayashi, Fumiki Komatsu, Fumi Murakami, Meng Zhao, et al.. A detailed paleomagnetic record between 2.1 and 2.75 Ma at IODP Site U1314 in the North Atlantic: Geomagnetic excursions and the Gauss-Matuyama transition. *Geochemistry, Geophysics, Geosystems*, 2012, 13, p. 410-432. 10.1029/2012GC004080 . insu-03583351

HAL Id: insu-03583351

<https://insu.hal.science/insu-03583351>

Submitted on 22 Feb 2022

HAL is a multi-disciplinary open access archive for the deposit and dissemination of scientific research documents, whether they are published or not. The documents may come from teaching and research institutions in France or abroad, or from public or private research centers.

L'archive ouverte pluridisciplinaire **HAL**, est destinée au dépôt et à la diffusion de documents scientifiques de niveau recherche, publiés ou non, émanant des établissements d'enseignement et de recherche français ou étrangers, des laboratoires publics ou privés.

Copyright



A detailed paleomagnetic record between 2.1 and 2.75 Ma at IODP Site U1314 in the North Atlantic: Geomagnetic excursions and the Gauss-Matuyama transition

Masao Ohno

Department of Environmental Changes, Faculty of Social and Cultural Studies, Kyushu University, Fukuoka 819-0395, Japan (mohno@scs.kyushu-u.ac.jp)

Tatsuya Hayashi

Department of Geology and Paleontology, National Museum of Nature and Science, Tsukuba, Ibaraki 305-0005, Japan

Fumiki Komatsu, Fumi Murakami, and Meng Zhao

Department of Environmental Changes, Faculty of Social and Cultural Studies, Kyushu University, Fukuoka 819-0395, Japan

Yohan Guyodo

Institut de Mineralogie et de Physique des Milieux Condenses, CNRS-UPMC-UPD-IPGP, F-75252 Paris CEDEX 05, France

Gary Acton

Department of Geology, University of California, Davis, California 95616, USA

Helen F. Evans

Lamont-Doherty Earth Observatory, Earth Institute at Columbia University, Palisades, New York 10964, USA

Toshiya Kanamatsu

Institute for Research on Earth Evolution, Japan Agency for Marine-Earth Science and Technology, Yokosuka, Kanagawa 237-0061, Japan

[1] This study investigated the detailed geomagnetic field variation between 2.1 and 2.75 Ma from a sediment core (IODP Site U1314) with high sedimentation rate (≥ 10 cm/kyr) and good age control. Characteristic remanent magnetization directions were well resolved by stepwise alternating field demagnetization. As a proxy of relative paleointensity, natural remanent magnetization (NRM) normalized by anhysteretic remanent magnetization (ARM) was used after testing that the influence of magnetic interaction in ARM is negligible. As a result, the following features of the geomagnetic field in the studied period have been revealed. During the transition of the Gauss-Matuyama (G-M) reversal and the Réunion Subchron, the paleointensity decreased to the value lower than 20% of the average intensity in the whole studied interval. In addition to these lows, eight paleointensity lows were found associated with large directional changes that satisfy the definition of a geomagnetic excursion. Four of these have ages close to ages reported for geomagnetic excursions in prior studies, whereas the other four excursions have not previously been observed. In our results, we confirm that the G-M transition occurred in marine isotope stage 103 even if we consider the shift in depth due to the lock-in process

of magnetic particles. The temporal variation in paleointensity showed asymmetric behavior associated with the G-M transition, with a gradual decrease prior to the transition and a rapid recovery after the transition.

Components: 8100 words, 11 figures, 1 table.

Keywords: Expedition 306; Integrated Ocean Drilling Program; Site U1314; geomagnetic excursion; paleomagnetic intensity; polarity transition.

Index Terms: 1513 Geomagnetism and Paleomagnetism: Geomagnetic excursions; 1521 Geomagnetism and Paleomagnetism: Paleointensity; 1535 Geomagnetism and Paleomagnetism: Reversals: process, timescale, magnetostratigraphy.

Received 30 January 2012; **Revised** 9 April 2012; **Accepted** 12 April 2012; **Published** 12 May 2012.

Ohno, M., T. Hayashi, F. Komatsu, F. Murakami, M. Zhao, Y. Guyodo, G. Acton, H. F. Evans, and T. Kanamatsu (2012), A detailed paleomagnetic record between 2.1 and 2.75 Ma at IODP Site U1314 in the North Atlantic: Geomagnetic excursions and the Gauss-Matuyama transition, *Geochem. Geophys. Geosyst.*, 13, Q12Z39, doi:10.1029/2012GC004080.

Theme: Magnetism From Atomic to Planetary Scales: Physical Principles and Interdisciplinary Applications in Geosciences and Planetary Sciences

1. Introduction

[2] Millennial-scale geomagnetic variations, such as polarity transitions and excursions, have been a focus of paleomagnetic studies, since they are essential elements in investigating geodynamo process. Paleomagnetic studies of sediment cores drilled from the ocean bottom have contributed to the study of such short time-scale variations.

[3] Much research in recent years has focused on paleointensity of the geomagnetic field for the past few million years. While sediments only yield the relative variations of the paleomagnetic field intensity, they possess the great advantage of providing continuous records, in contrast with absolute paleointensity records obtained from igneous rocks [e.g., Guyodo and Valet, 1999a]. By stacking relative paleointensity data from various areas, global paleointensity variation has been studied at millennial time scales. Guyodo and Valet [1999b] stacked 33 records of relative paleointensity into a composite curve spanning the past 800 kyr (Sint-800) and found that the intensity of the Earth's dipole field has experienced large-amplitude variations over this period. Valet *et al.* [2005] extended the record back to 2 Ma; they stacked 10 records into a composite record (Sint-2000). Channell *et al.* [2009] produced a well-dated stack of 13 paleointensity records encompassing the past 1.5 Myrs, with only 6 records covering the entire time interval. Between 2 and 3 Ma, only a few paleointensity records [Valet and Meynadier, 1993; Kok and Tauxe, 1999; Yamazaki and Oda, 2005] have

been reported (see review by Tauxe and Yamazaki [2007]). All these paleointensity records [Valet and Meynadier, 1993; Kok and Tauxe, 1999; Yamazaki and Oda, 2005] were obtained from sediment cores in equatorial Pacific with relatively low average sedimentation rates of 0.5–2.5 cm/kyr.

[4] A geomagnetic excursion is a short-term large directional change often associated with low paleointensity. A geomagnetic excursion is defined by a paleomagnetic direction that gives a virtual geomagnetic pole (VGP) that deviates significantly from the paleogeographical poles, where significantly is usually taken to be 45° or 40° of angular distance [e.g., Laj and Channell, 2007]. Many geomagnetic excursions have been reported, and it often happens that a geomagnetic excursion occurring in a sediment core drilled at a specific location is not found in a sediment core from another location. No consensus has been reached as to the number of excursions that have occurred even within the Brunhes Chron, for which by far more detailed studies have been made relative to older periods. In a review by Oda [2005], 23 excursions were identified in the Brunhes Chron, and 18 out of them were considered to be reliably determined and dated. Lund *et al.* [2006] provided evidence for 17 Brunhes-age excursions from ocean drill cores. Laj and Channell [2007] listed 12 excursions in the Brunhes Chron, including seven that were considered to be well documented whereas the existence of the other five was considered to be less certain. Prior to the Brunhes Chron, the number of reported excursions decreases with age. In the Matuyama

Chron, *Laj and Channell* [2007] listed 10 excursions and only two of them are prior to the Réunion Subchron. They reported that there are no well-documented excursions in the Gauss Chron.

[5] The duration of a geomagnetic polarity transition is the period during which the geomagnetic field changes from one polarity (normal or reverse) to the opposite. *Merrill and McFadden* [1999] reviewed geomagnetic transitions recorded in sediments, igneous rocks, and sedimentary rocks. They concluded that the duration of a typical polarity transition lies in 1,000–8,000 years, with individual estimates ranging between about 10^2 and 2×10^4 years. *Clement* [2004] analyzed sediment records of the four most recent reversals (the Matuyama-Brunhes, the upper and the lower Jaramillo, and the upper Olduvai reversals) and estimated the average value to be about 7,000 years. As for the Gauss-Matuyama (G-M) transition, estimates of the duration of about 8–10 kyr are reported by *Glen et al.* [1999] and *Zhu et al.* [2000].

[6] In addition to the interest of the nature of the geomagnetic field itself, the age of geomagnetic polarity transition is important because polarity boundaries play a vital role in stratigraphic studies. The age of the latest reversal, the Matuyama-Brunhes (M-B) transition, is fairly well established to be 0.780 Ma [*Cande and Kent*, 1995], with an uncertainty of only about ± 0.01 Ma owing to dating uncertainties as well as the duration of the M-B transition that is complicated by a precursor event [*Dreyfus et al.*, 2008; *Channell et al.*, 2010]. In contrast, much larger uncertainty remains in the age of the Gauss-Matuyama (G-M) transition and its duration. In commonly used timescales, the age of the G-M transition is quoted as 2.581 Ma based on marine magnetic anomaly data and astronomical tuning, which place the reversal within marine isotope stage (MIS) 103 [*Cande and Kent*, 1995; *Lourens et al.*, 2004]. More recently, *Lisiecki and Raymo* [2005] estimated the age of G-M transition from marine sediment cores with oxygen isotope ages to be 2.608 Ma and to occur in MIS 104 (in Figure 4 of *Lisiecki and Raymo* [2005] the G-M transition occurs in MIS 104 although they assign G2 to the G-M transition in their Table 4, which was a typographical error as noted at <http://lorraine-lisiecki.com/stack.html>).

[7] The above discrepancies associated with short-term geomagnetic variation, such as in the number of geomagnetic excursions in the Brunhes Chron and in the age of the G-M polarity transition, arise partly from low sedimentation rate of the studied sediments and from the magnetization lock-in

process [e.g., *Guyodo and Channell*, 2002]. Geomagnetic excursions are smoothed out in sediments with low sedimentation rate and a minimum sedimentation rate of 10 cm/kyr has been suggested to consistently detect geomagnetic excursions on the basis of model calculation [*Roberts and Winklhofer*, 2004]. Concerning the age of polarity reversals recorded in sediments, the delay of age due to the lock-in process of magnetic particles must be considered. The depth at which the sediments acquire magnetization is a sum of surface mixing layer depth and a lock-in depth [*Roberts and Winklhofer*, 2004]. The surface mixing layer produces an apparent age offset for the occurrence of a magnetic polarity transition, while the lock-in depth controls the apparent length of the transition [e.g., *Channell and Guyodo*, 2004]. In sediments with a sedimentation rate of, for example, 1 cm/kyr, the delay of age extends as long as 20 kyr for a plausible depth of 20 cm to acquire magnetization [e.g., *Channell and Guyodo*, 2004; *Liu et al.*, 2008; *Suganuma et al.*, 2010].

[8] In this paper we present a record of paleomagnetic direction and relative intensity from a sediment core of high sedimentation rate (≥ 10 kyr/cm) at 2.1–2.75 Ma with good age control. We discuss the characteristics and the age of geomagnetic excursions in this period and of the G-M polarity transition.

2. Sampling and Magnetic Measurement

[9] Integrated Ocean Drilling Program (IODP) Site U1314 was drilled in the Gardar Drift at 56°21.9'N, 27°53.3'W in a water depth of 2820 m (Figure 1). Three holes (Holes A, B, and C) were drilled with the advanced piston corer (APC) using non-magnetic core barrels; the core recovery was nearly 100% with the quoted rate, which is influenced by core expansion, exceeding 100% at each hole [*Expedition 306 Scientists*, 2006]. A complete spliced section was obtained down to 280 m composite depth (mcd). Note that the mcd in this paper is shifted up by 0.9 m relative to the shipboard mcd for depths greater than 260.0 mcd [see *Hayashi et al.*, 2010, Appendix B]. Only one lithologic unit is defined at IODP Site U1314 which consists of nannofossil- and clay-rich sediments [*Expedition 306 Scientists*, 2006].

[10] Onboard the ship natural remanent magnetizations (NRMs) of 'archive' half core were measured applying alternating field (AF) demagnetization of up to 20 mT peak field. Most of the drill-string

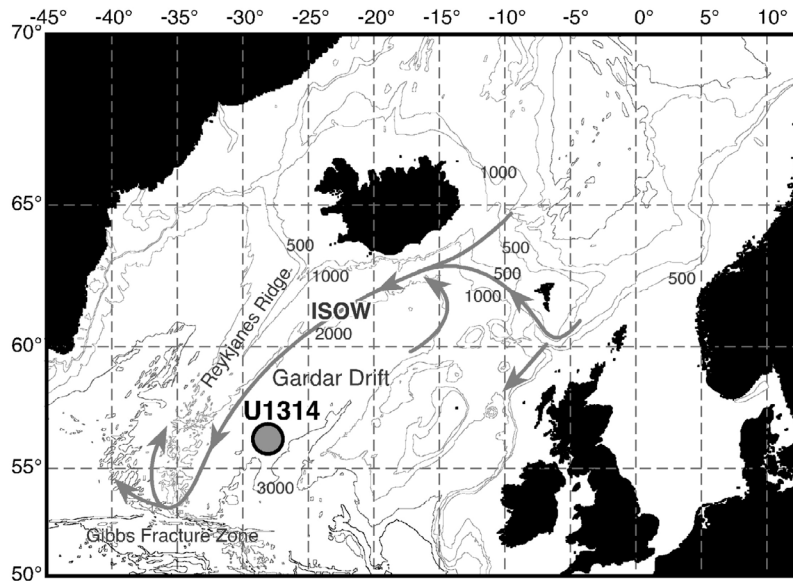


Figure 1. Location map for IODP Site U1314 in the Gardar Drift. Bathymetric contours in meters.

overprint, which was downward in direction, was removed at around 10 mT during onboard treatment [Expedition 306 Scientists, 2006]. For further high-resolution measurements, u-channel samples of 1.5 m in length with 2×2 cm square cross section were sampled from the central part of these ‘archive’ half cores at Bremen Core Repository. In addition, u-channel samples were collected from the ‘working’ half of other holes (i.e., other than the hole included in the spliced section) in intervals where shipboard NRM measurements showed large inclination anomalies, which may indicate geomagnetic excursions. Remanent magnetizations were measured at Center for Advanced Marine Core Research in Kochi University. The NRM of the u-channel samples were measured at every 1 cm interval using a high-resolution small-access pass-through magnetometer (2G Enterprises, 755SRM) after AF demagnetization in 10 steps in the 20–80 mT interval for archive halves and 14 steps in the 0–80 mT interval for working halves, respectively. The declination values were corrected according to the shipboard ‘Tensor Multishot’ orientation tool. Subsequently anhysteretic remanent magnetization (ARM) was imparted in an 80 mT AF with 0.1 mT DC biasing field. The ARM was also measured after AF demagnetization stepwise up to 60 mT. The NRM record in 2.57–2.60 Ma (238–243 mcd) including the G-M Transition has been previously published [Ohno *et al.*, 2008]; the other paleomagnetic results are newly reported in the present paper.

[11] Rock magnetic studies of the U1314 sediments have already been reported [Zhao *et al.*, 2011; Hayashi *et al.*, 2010]. Low-temperature and high-temperature magnetometry indicated magnetite as the dominant magnetic mineral [Zhao *et al.*, 2011]. The hysteresis ratios concentrated closely in the pseudo-single domain (PSD) field [Hayashi *et al.*, 2010].

[12] In converting the depth in core into age, we used the age model of Hayashi *et al.* [2010]. They constructed a hybrid environmental proxy ($\chi + \text{NGR}$) of the U1314 sediments by combining magnetic susceptibility (χ) and natural gamma radiation (NGR), in which glacial-interglacial variations are extracted and the small-scale variations (attributed to ice-rafted debris) are eliminated. They established the age model during the period 2.1~2.75 Ma by tuning the hybrid environmental proxy record to the global-standard oxygen isotope curve [Lisiecki and Raymo, 2005].

[13] In the present paper, we report the paleomagnetic results between 188.0 mcd and 262.5 mcd of the core that corresponds to the age between 2.1 Ma and 2.75 Ma. As shown in the age-depth curve (Figure 2), the sedimentation rate is generally as high as between 10 and 20 cm/kyr.

3. Results

[14] As seen in the orthogonal projection of the results of AF demagnetization of NRM (Figure 3), a

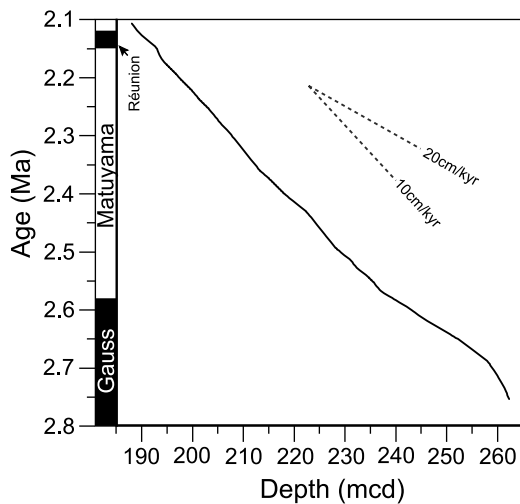


Figure 2. Age-depth plot modified after Hayashi *et al.* [2010] (solid curve). The slope of the dashed lines indicates the sedimentation rate.

well defined characteristic magnetization component which goes straight to the origin of the plot was generally obtained for the 20–80 mT demagnetization intervals. We determined the characteristic direction applying principal component analysis [Kirschvink, 1980] for each measurement point using a computer program developed by Mazaud [2005]. Figure 4 shows the change in characteristic direction with age. In general, we used all ten steps in the 20–80 mT AF demagnetization range in the principal component analysis. The maximum angular dispersion (MAD) values are generally low ($<1^\circ$), indicating the characteristic directions are well defined. In case the MAD value exceeded 10° , the orthogonal plot was examined individually and the principal component was determined using at least seven of the ten measurement steps (see e.g., Figure 3c). As mentioned earlier, the declination was corrected according to the shipboard ‘Tensor Multishot’ orientation tool. After this correction, however, the average declination in each core was apart from the direction of the geographic poles (0° or 180°) by up to 45° . Although part of the deviation may be related to geomagnetic field variability, when it is so large much of the deviation probably results from uncertainties in core orientation. Such large systematic errors are known to arise in orienting IODP piston cores. These can be caused by failure to get a stable orientation estimate while the ‘Tensor Multishot’ tool is in the hole, magnetic interference from drilling equipment, uncertainty in aligning the orientation tool with the scribe lines on the core liner, and possible twisting of the core relative to the core liner as the piston core is shot.

Because these deviations are unlikely geomagnetic in origin, we have corrected the declination by rotating the core so that the calculated core-average declination is oriented North or South for positive and negative inclination interval, respectively. In Figure 4 we plot the declination before (red) and after (black) this correction. In calculating the average declination, we excluded the declination values that differ from the calculated average by more than $\pm 45^\circ$ by performing an iterative calculation. We did not apply this correction to the cores A24H (2494–2548 ka) and A25H (2577–2612 ka, which includes G-M transition) because the correction was negligibly small (less than 5°). We note that evidence for core twisting was found to be absent or negligible within the uncertainties based on comparing the declination between holes through the studied interval.

[15] A relative paleointensity proxy was generated by normalizing NRM by ARM (Figure 5). We calculated the slopes of the NRM intensity versus ARM intensity plot by applying linear regression to all the measurement points of the AF demagnetization steps in the 20–80 mT peak field range. In Figure 5, linear correlation coefficient (r) provides a measure of the uncertainty in linear regression of the slope. The correlation coefficients are generally high (>0.99) indicating that relative paleointensity values are well defined. Several spikes of low values occur in the correlation coefficients corresponding to low values in relative paleointensities. In these intervals, a large directional change is usually observed with large MAD values. Large MAD values and low correlation coefficients are partly attributed to the relatively low NRM intensity (relatively high noise). Overprinting of rapidly changing geomagnetic field may also increase the MAD values and decrease the correlation coefficients [Channell *et al.*, 2002].

[16] In general, the normalizer used in determining a paleointensity proxy is either ARM or IRM (isothermal remanent magnetization). We used ARM as a normalizer to obtain a proxy for relative paleointensity in Figure 5 because we could not obtain the IRM record of U1314 sediments. The IRM of the sediments in the present study is too strong to measure with a SQUID magnetometer. Since acquisitions of ARM are influenced by magnetic interactions among magnetic particles [Yamazaki, 2008], IRM is usually preferred as a normalizer, particularly for sediments in the Pacific [Yamazaki, 2008; Yamazaki and Oda, 2005; Yamamoto *et al.*, 2007b]. The sediments in the north Atlantic generally do not show much difference

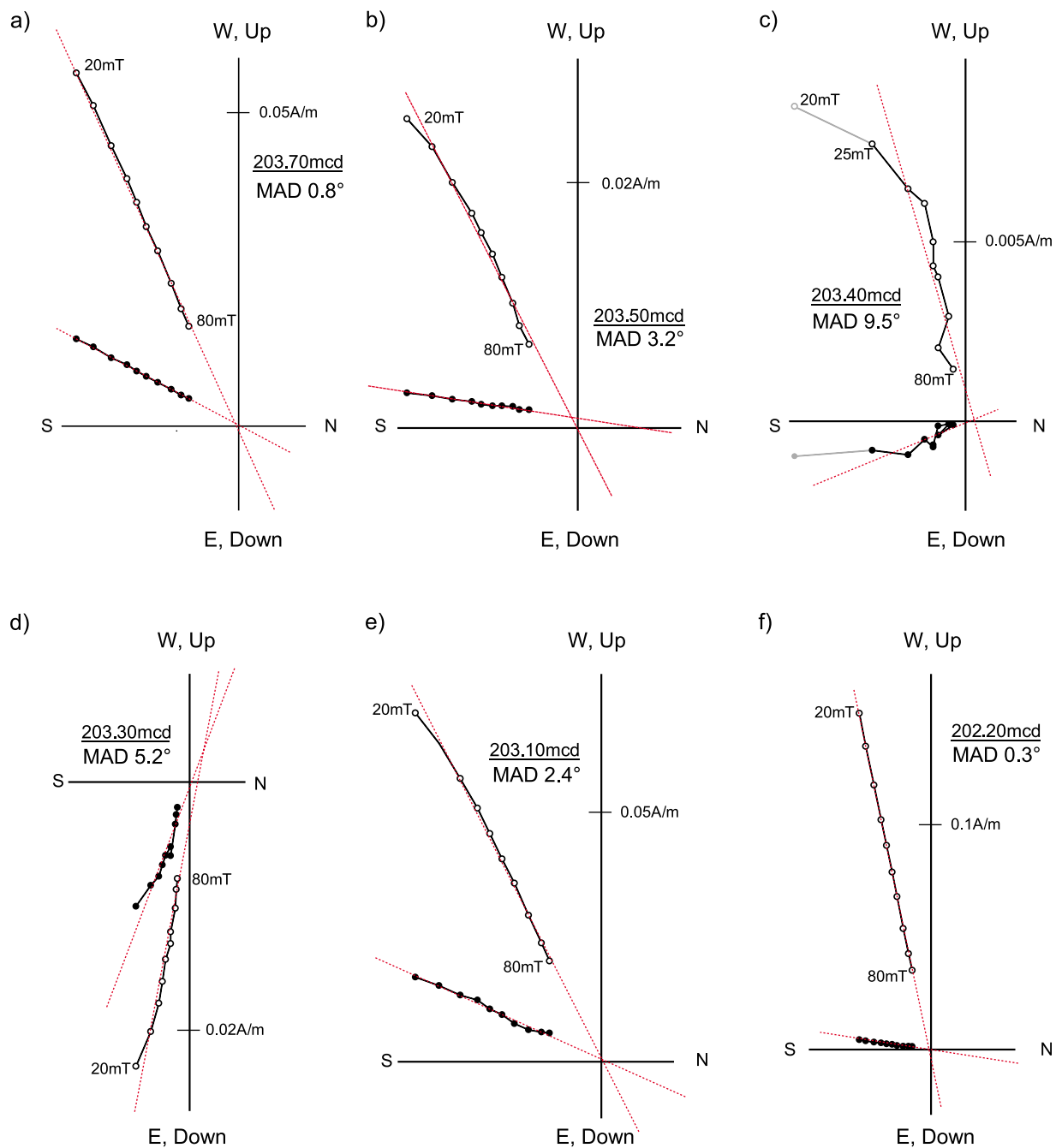


Figure 3. Examples of orthogonal projections of alternating field demagnetization. Solid circles represent horizontal projection, and open circles represent vertical projection. The point that was excluded in calculating the characteristic direction is denoted in gray color. Peak alternating field (mT) for some demagnetization step is indicated. Dotted lines indicate the calculated characteristic directions.

between NRM normalized by ARM (hereafter, NRM/ARM) and NRM normalized by IRM (hereafter, NRM/IRM); as a proxy of relative paleointensity, NRM/ARM is used in some papers [Channell *et al.*, 2002; Channell and Raymo, 2003; Channell, 2006; Channell *et al.*, 2008] and NRM/IRM is used in others [Channell *et al.*, 1997;

Channell, 1999; Channell and Kleiven, 2000; Channell *et al.*, 2003, 2004].

[17] We completed two tests to check if the ARM of the sediments in the present study is influenced by magnetic interactions. First, we show the plot of NRM/ARM against ARM in Figure 6. If ARM

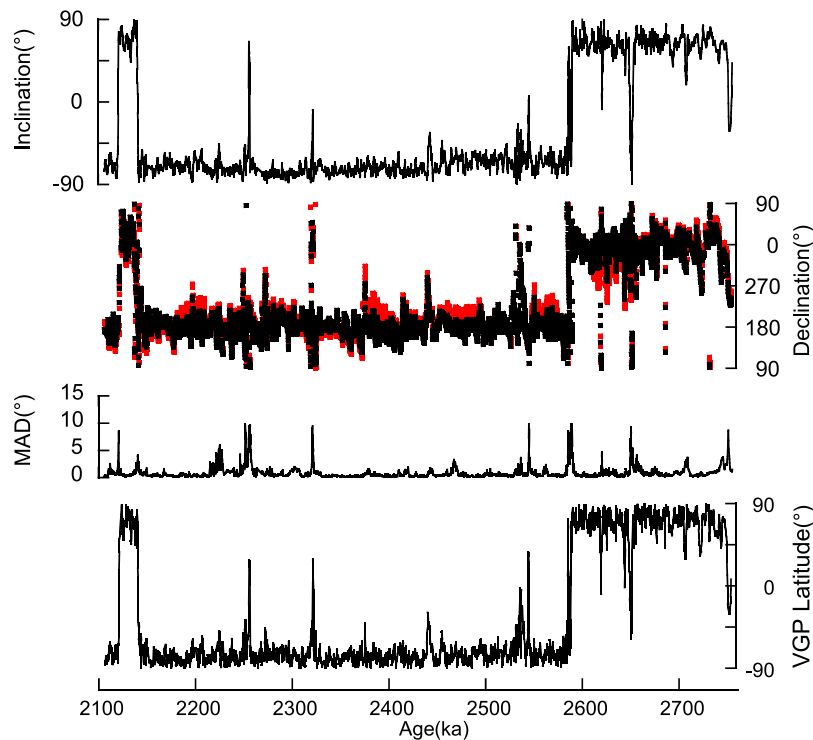


Figure 4. Characteristic directions (declination and inclination), maximum angular dispersion (MAD) and the latitude of virtual geomagnetic pole (VGP).

saturates because of the influence by magnetic interaction, NRM/ARM would increase with increase of ARM. However, any trend of NRM/ARM with increase of ARM is not observed in

Figure 6. Spectral methods such as cross-coherence [Tauxe, 1993] and wavelet analysis [Guyodo *et al.*, 2000] have become common tools to further test the quality of relative paleointensity records. We

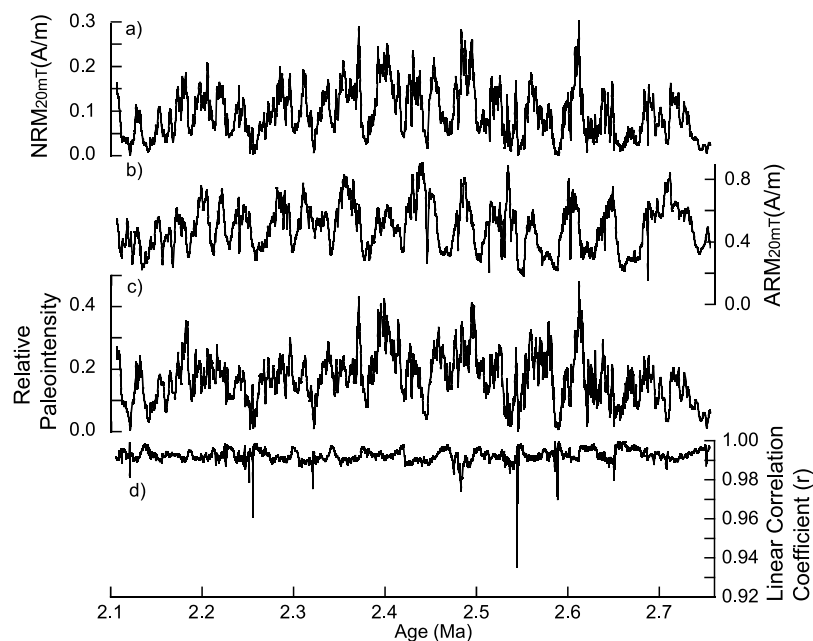


Figure 5. (a) Natural remanent magnetization (NRM) and (b) anhysteretic remanent magnetization (ARM) after alternate field demagnetization of 20 mT. (c) Relative paleointensity and (d) linear correlation coefficient (see text).

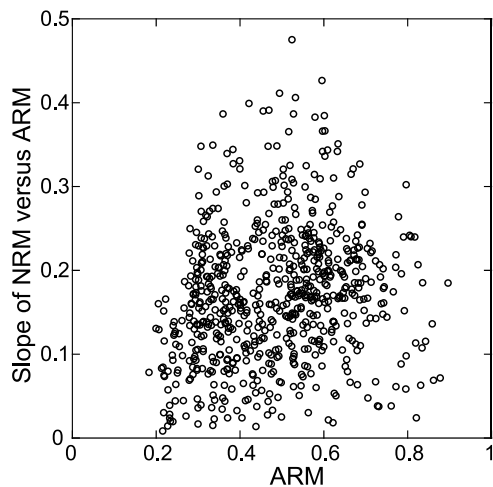


Figure 6. Plot of paleointensity proxy (slopes of NRM intensity versus ARM intensity plot) against ARM at every 10 cm. Both NRM and ARM are after alternate field demagnetization of 20 mT.

therefore calculated the wavelet coherence [Grinsted *et al.*, 2004] between NRM/ARM and ARM. In the wavelet power spectrum of ARM (Figure 7a), a strong power at a period of 41 kyr is prominent implying the presence of climatic cycle in the ARM record. In the wavelet coherence between ARM and NRM/ARM in Figure 7b, no coherence is observed at a period of 41 kyr corresponding to the strong power of ARM. As a result of these tests, the influence of magnetic interaction in the present sediments is negligible and does not lower the quality of NRM/ARM as a paleointensity proxy.

[18] We summarize the paleomagnetic direction and the relative intensity of U1314 in Figure 8, together with the tuning material ($\chi + \text{NGR}$) and the tuning target (LR04) used in determining the age model in Hayashi *et al.* [2010]. Prior to MIS 85, the correlation between the tuning material ($\chi + \text{NGR}$) and the tuning target (LR04) is excellent, which guarantee the reliability of age in this period. The correlation between these parameters is lower in the period younger than MIS 85, in which the Réunion Subchron occurred. Therefore, we do not discuss the age and the duration of the Réunion Subchron in this paper.

4. Discussion

4.1. Paleointensity Lows and Geomagnetic Excursions

[19] In Figure 8, the gray bars indicate the layer whose relative paleointensity dropped to less than

30% of the average value in the whole studied interval. During the Gauss-Matuyama (G-M) transition and the top and the bottom Réunion transitions, the paleointensity dropped to less than 20% of the average value. In addition to them, eight paleointensity lows were observed and labeled from L1 to L8.

[20] All the labeled paleointensity lows (L1–L8) are associated with large directional changes. For the layers at which the large fluctuations of inclination was found in the spliced section, we measured the same stratigraphic level from other holes: for example, if the inclination anomaly occurred in Hole U1314A from the spliced section, we confirmed its occurrence by also measuring the paleomagnetic direction for the same interval in

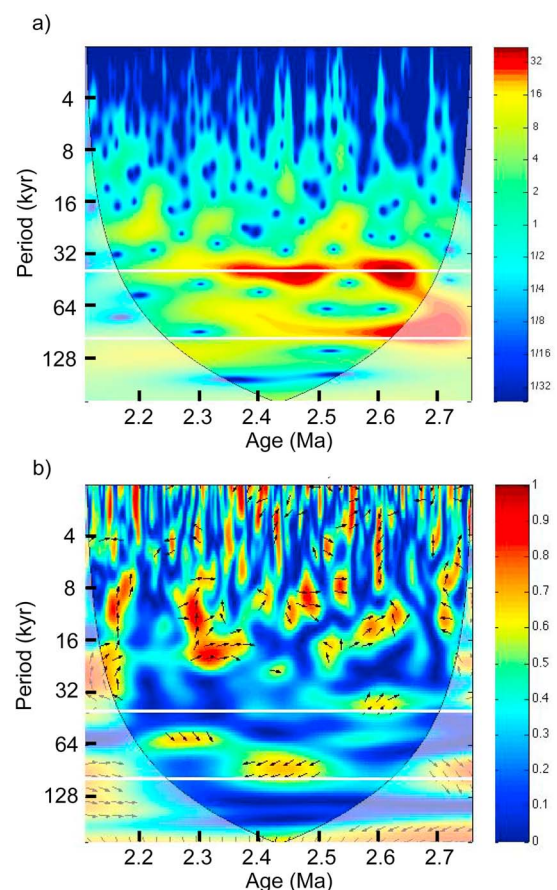


Figure 7. Results of wavelet analysis: (a) Wavelet power spectrum of ARM and (b) wavelet coherence between the paleointensity proxy (slopes of NRM intensity versus ARM intensity plot) and ARM. The white-shaded areas show the cone of influence in which edge effect due to ends of the signals cannot be ignored. Two horizontal white lines indicate periods of 41 and 100 kyr, respectively.

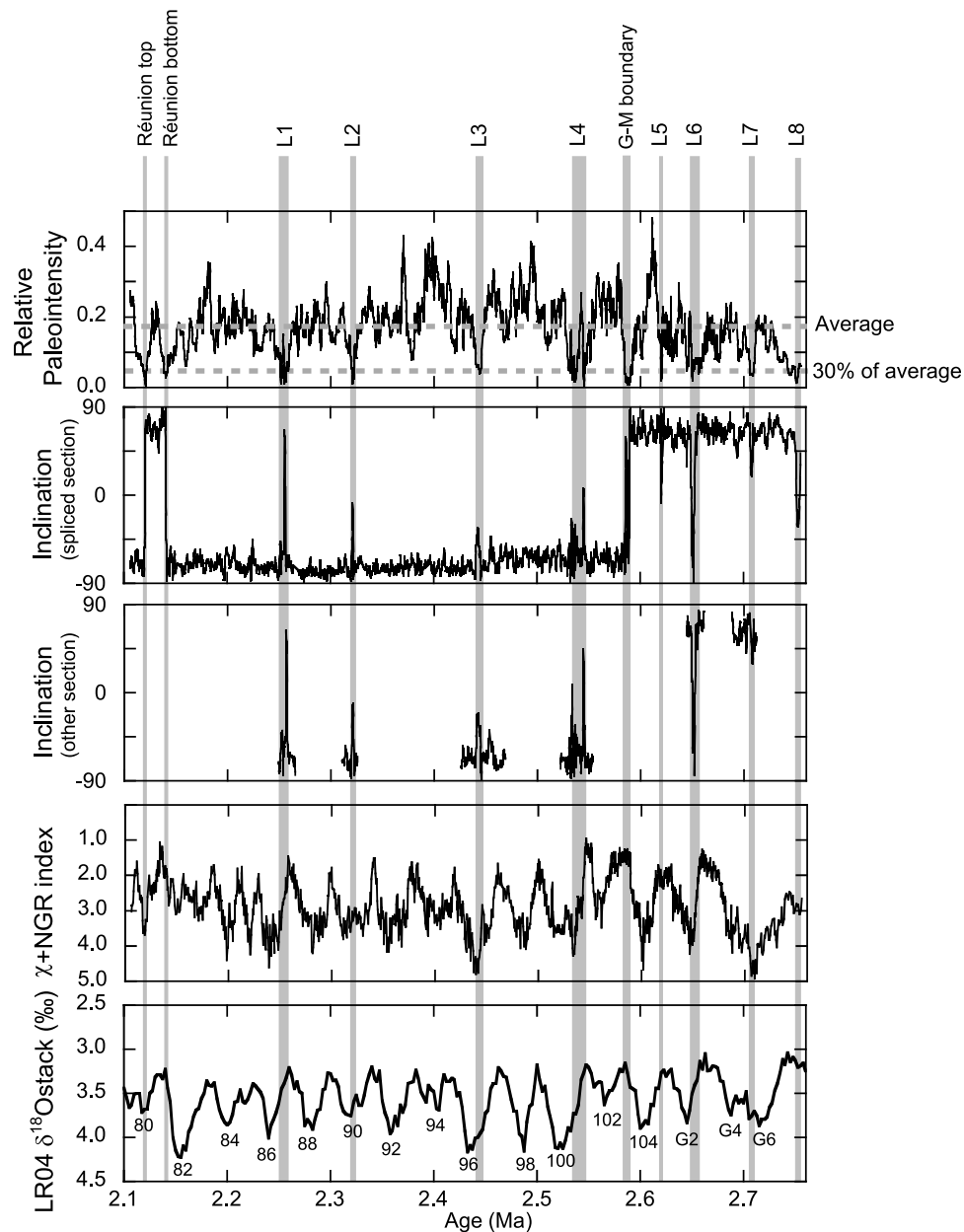


Figure 8. Summary of paleomagnetic results (relative paleointensity in arbitrary unit, inclination from spliced sections, inclination from other holes than spliced sections) together with tuning material ($\chi + \text{NGR}$) and tuning target (oxygen isotope curve, LR04) in the age determination. Numerals in LR04 plot are the numbers of marine isotope stage. The gray bars indicate paleointensity lows (see text).

either Hole U1314B or C. As a result, the same or very similar large directional changes were confirmed to exist in two coeval cores (Figure 8). These large directional changes are, therefore, not caused by disturbance during drilling or sampling. Furthermore, the hysteresis parameters of the sediments sampled from the depth that showed large directional changes do not differ from those of other depths in the Day plot (Figure 9). In addition, we did

not find any changes related to these layers in ARM record. These results support that the paleointensity lows and the associated directional changes of these layers are not caused by lithologic inhomogeneities.

[21] The U1314 paleointensity record correlates well with other coeval records [Valet and Meynadier, 1993; Kok and Tauxe, 1999; Yamazaki and Oda, 2005], with the correlation to the EPAPIS-3Ma record (equatorial Pacific paleointensity stack

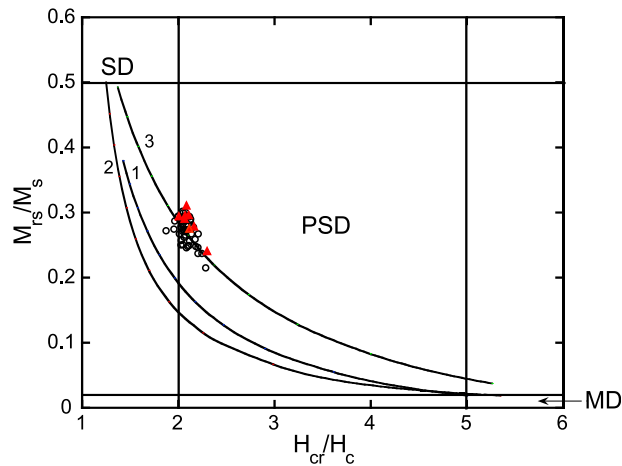


Figure 9. Day et al. [1977] plot of the hysteresis parameters: M_{rs} , saturation remanence; M_s , saturation magnetization; H_{cr} , remanent coercivity; H_c , coercive force. SD, PSD and MD indicate single domain, pseudo single domain and multidomain fields, respectively, with the limits in Dunlop [2002a]. Curves 1–3 are theoretical SD + MD mixing curves from Dunlop [2002a, 2002b]. Results of samples from layers of geomagnetic excursions are denoted by red triangles while others are denoted by open circles.

[Yamazaki and Oda, 2005]) being excellent. The correlation is not affected much by the new age model for EPAPIS-3Ma (details of the new age model are provided in Appendix A). The record of EPAPIS-3Ma in this period is a stack of relative paleointensity records of three cores drilled at equatorial Pacific. The lows in the U1314 paleointensity record except L5 corresponds one-to-one to those in EPAPIS-3Ma in Figure 10. In addition to the labeled lows in U1314 paleointensity record, a minimum of 45% of the average at 2.38 Ma of U1314 record is also found in EPAPIS-3Ma. This marked correlation between cores in the Atlantic and the Pacific strongly supports that these records represent change in global geomagnetic intensity. The record of OJP-stack [Kok and Tauxe, 1999] in this period is a stack of relative paleointensity records of two cores. In comparison with OJP-stack, as Yamazaki and Oda [2005] described, several lows are correlative with slight shifts in age. The correlation is rather poor between the record of ODP Leg 138 [Valet and Meynadier, 1993] and the present result.

[22] Despite the relatively good correlation between U1314 and EPAPIS-3Ma records, the paleointensity lows in EPAPIS-3Ma are older than those in U1314 by about 20 kyr in average. This is explained by the higher sedimentation rate of U1314 sediments (≥ 10 cm/kyr) than that of EPAPIS-3Ma

sediments (0.5–1 cm/kyr). The delay of 20 kyr corresponds to a shift in depth of 10–20 cm for EPAPIS-3Ma. The depth of 10–20 cm is consistent with the estimate of the depth at which the magnetic particles are locked-in in marine sediments [e.g., Channell and Guyodo, 2004; Liu et al., 2008; Saganuma et al., 2010]. For the sediments of U1314, such delay in acquisition of remanence is estimated to be 1–2 kyr if we assume its thickness to be ~ 20 cm. Another difference between these records is their smoothness. The paleointensity lows in EPAPIS record are not as deep as those in U1314 record, which is also explained by low sedimentation rate of EPAPIS-3Ma record; the sharp geomagnetic variation is smoothed in sediments of low sedimentation rate. The EPAPIS-3Ma record is also smoothed as a result of stacking (averaging) of three records.

[23] The ages and corresponding marine isotope stages (MIS) of L1–L8 are tabulated in Table 1. The VGPs during the period of paleointensity lows, other than L3 and L5, crossed the equator to the opposite hemisphere (Figure 4). The VGPs during the period of L3 and L5 also approached close to the equator, deviating from the geographical pole by well in excess of 45° . Hence, all these directional changes at L1–L8 fall in the category of a geomagnetic excursion. The duration, which we defined in this paper as the intervals with the VGP further than 45° from the geographic poles, was generally a few thousand years in Table 1. The duration of L4 is as long as 11 kyr, but the directional change of L4 consists of three spikes; the duration of each spike is a few thousand years. In addition to the geomagnetic excursions at L1–L8, the VGP falls slightly further than 45° from the geographic pole at 2.38 Ma, 2.69 Ma, and 2.72 Ma. Since the large fluctuation of VGP at these ages originates in declination change and the inclination change is not very large, the position of VGP depends largely on the correction in declination in which we set the average declination to the poles as described earlier. The large short-term change in declination is real, however, even if the absolute core-mean declination is known only imprecisely. Given the relative small inclination change and the lack of absolute mean declination, we are unsure that the apparent geomagnetic excursions at 2.38, 2.69, and 2.72 Ma have a pure geomagnetic origin and therefore do not include them in the following discussion.

[24] In Table 1, we compare the ages of excursions L1–L8 with other geomagnetic excursions reported in 2.2–2.8 Ma age range. Yang et al. [2007] reported

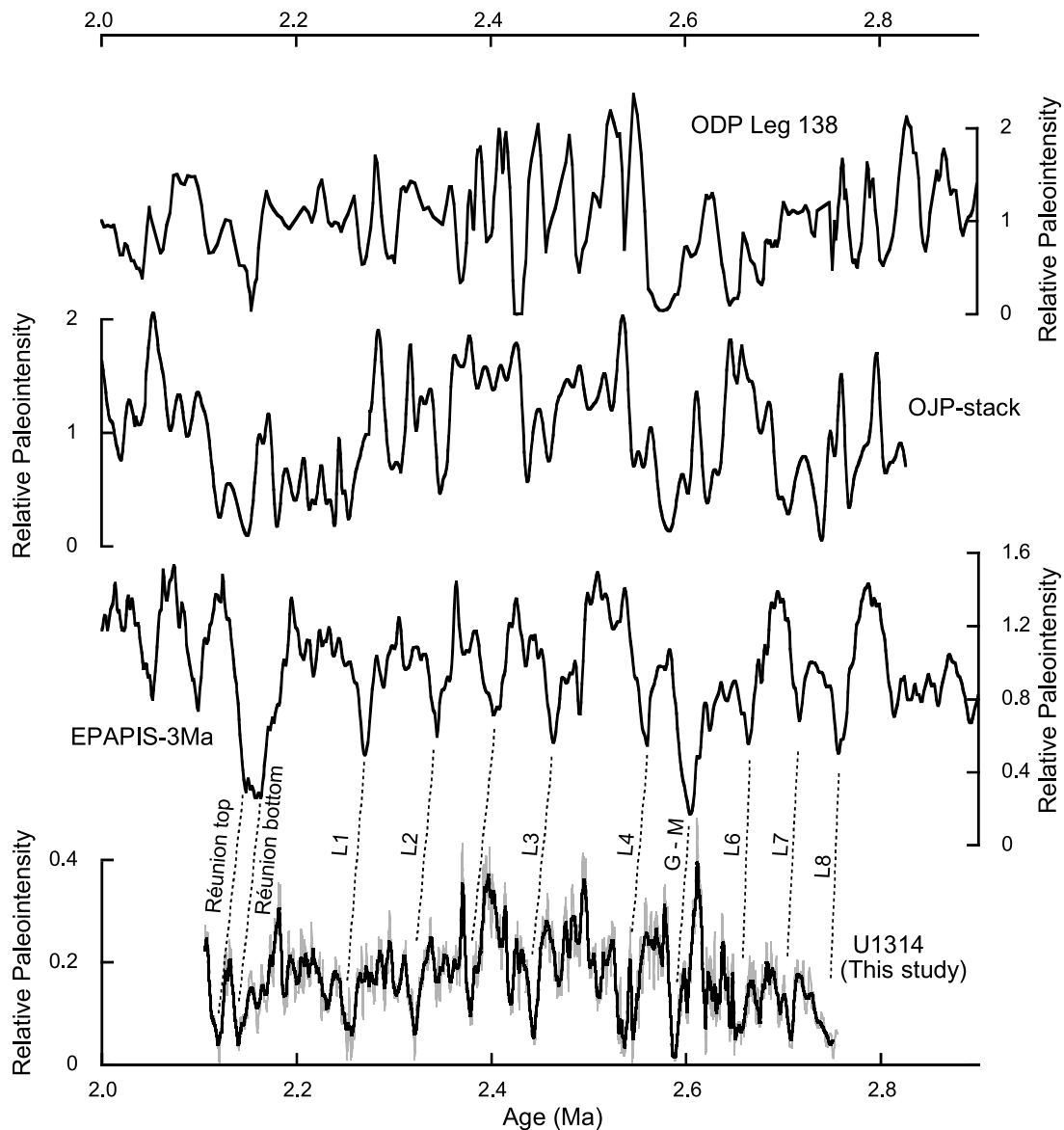


Figure 10. Comparison of relative paleointensity records; U1314 record (this study), EPAPIS-3Ma record [Yamazaki and Oda, 2005], OJP-stack record [Kok and Tauxe, 1999], and the record of ODP Leg 138 [Valet and Meynadier, 1993]. The black line of U1314 record is the smoothed (40 cm running average) line and the gray line is the original data (see text).

three excursions in this period from Chinese Loess Plateau. *Cande and Kent* [1995] reported a cryptochron at 2.42–2.44 Ma based on ‘tiny wiggles’ in marine magnetic anomaly data. In *Channell and Guyodo* [2004] two excursions are found from a sediment core nearby Site U1314. As noted in the Table 1, some of these previously noted excursions may be the same as the excursions observed at Site U1314; the difference in age is up to 30 kyr, which falls within dating uncertainties. *Yamamoto et al.* [2007a] reported an excursion from volcanic rocks in Society Islands; the error of its age overlaps the age of L8. In the studied period, no excursions older than

the age of L3 have been reported from marine sediments. This may be attributed to the higher sedimentation rate of U1314 relative to other cores in this period. Hence, we believe the observed changes (L1–L8) reflect the true geomagnetic field, and that future paleomagnetic studies of other sedimentary sections with similar or higher sedimentation rates will confirm the existence of these eight excursions.

4.2. Gauss Matuyama Polarity Transition

[25] Geomagnetic polarity transitions play an important role in stratigraphic study in addition to

Table 1. Geomagnetic Excursions and Chryptochrons

Chinese Loess ^a		GPTS ^b		ODP Site 982 ^c		Volcanic Rocks ^d : Age (Ma)	This Study			
Name	Age (Ma)	Name	Age (Ma)	MIS	Age (Ma)		Name	MIS	Age (Ma)	Duration (kyr)
E5	2.25			85/86	2.24		L1	86/87	2.25	1
E6	2.35						L2	90	2.32	1
E7	2.42	C2r.2r-1	2.42–2.44	95	2.42		L3	96	2.44	2
							L4	100/101	2.53–2.55	11
							L5	105	2.62	1
							L6	G2/G3	2.65	4
							L7	G5/G6	2.71	2
						2.77 ± 0.02	L8	G7	2.75	4

^aYang et al. [2007].

^bCande and Kent [1995].

^cChannell and Guyodo [2004].

^dYamamoto et al. [2007a].

the interest of the behavior of the geomagnetic field during transitions. The age of G-M polarity transition falls in MIS 103 in the oxygen isotope curve in Figure 8. As discussed earlier, the delay in age due to post depositional lock-in of magnetic particles is estimated to be up to 20 cm; that is the true depth of transition is shallower than the present depth by up to 20 cm. Even if we shift the depth of transition up by 20 cm, it remains within MIS 103. As for the absolute age of the transition, in Figure 11, the

VGPs are located near the north geographical pole (>45°N) until 2.590 Ma, and deviate between the north and south geographical poles until stabilizing near the south geographical pole at 2.585 Ma. The above shift in the depth of transition up by 20 cm corresponds to shift in age to younger one by 1 kyr because the sedimentation rate at this depth is nearly 20 cm/kyr (Figure 11). In addition, the age may include an error of up to ±5 kyr because the age model is constructed by matching the 41-kyr

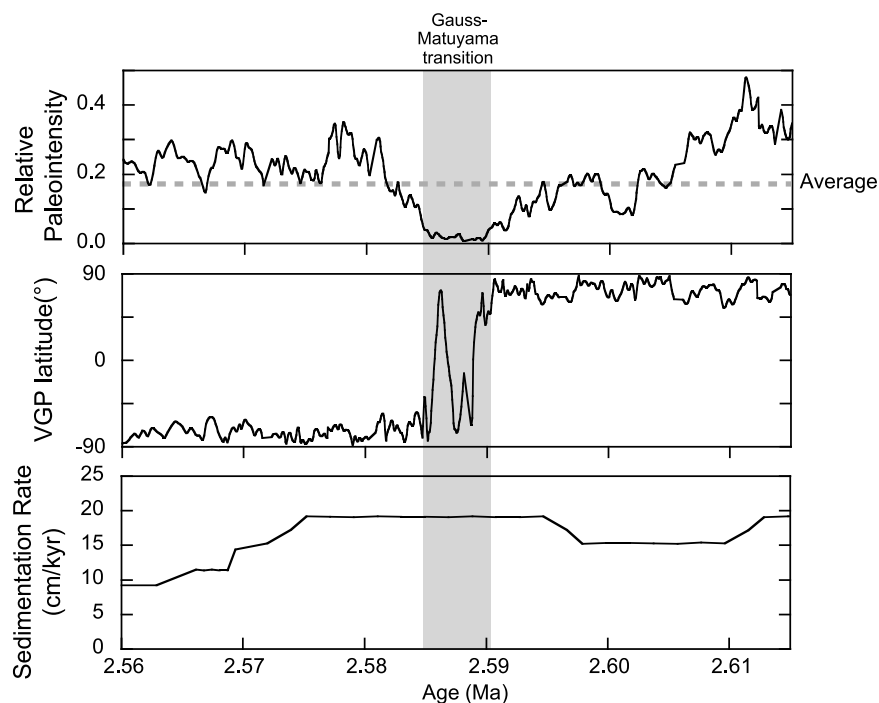


Figure 11. Relative paleointensity, the latitude of VGP, and the sedimentation rate of Site U1314 for the period including the G-M polarity transition.

periodicities in environmental variations. Hence, a best estimate for the G-M transition is 2.587 Ma with an uncertainty that is at least ± 5 kyr.

[26] Our age estimate for the G-M transition is close to the value 2.581 Ma estimated from marine magnetic anomaly data by *Cande and Kent* [1995]. In contrast, *Lisiecki and Raymo* [2005] obtain an age of 2.608 Ma, which is in MIS 104. We suggest this age estimate is older by about 20 kyr as a result of post-depositional lock-in within the slow sedimentation rate of the cores that *Lisiecki and Raymo* [2005] included in their analysis.

[27] *Deino et al.* [2006] obtained a $^{40}\text{Ar}/^{39}\text{Ar}$ age of 2.589 ± 0.003 Ma for G-M boundary from lacustrine sediments in Kenya. They adjusted the $^{40}\text{Ar}/^{39}\text{Ar}$ age by 0.8% to 2.610 Ma by calibrating the dating standard on the basis of the $^{40}\text{Ar}/^{39}\text{Ar}$ age of an astronomically dated ash layer at ca. 7 Ma [*Kuiper et al.*, 2004]. This calibrated age (2.610 Ma, which is in MIS 104) is 28 kyr older than the age (2.582 Ma, which is in MIS103) directly determined by astronomical calibration at the layer that includes G-M transition [*Lourens et al.*, 1996]. Lock-in delay of NRM acquisition in the lacustrine sediments in Kenya is not a plausible explanation for the delay of 28 kyr because of the high sedimentation rates. Therefore, the discrepancy in the astronomically calibrated ages suggests some inconsistency in astronomical tuning. Our result is consistent with the directly determined age, which suggests a possibility of problem in the age calibration in *Deino et al.* [2006].

[28] The estimated duration of the G-M transition is 5 kyr (Figure 11), which is within the duration of a typical geomagnetic polarity transition of 1–8 kyr reviewed by *Merrill and McFadden* [1999]. The definition of duration, which determines the duration as the interval at which VGPs fall more than 45° away from the geographical poles, gives the lower limit of duration in *Clement* [2004]. In other studies of G-M transition, *Zhu et al.* [2000] estimated the total duration to be 9–10 kyr in China (34.2°N , 109.2°E). The duration of G-M transition in the U.S.A. (35.7°N , 242.6°E) by *Glen et al.* [1999] is about 8 kyr in their Figure 4. *Burakov et al.* [1976] estimated the duration of the G-M transition to be 10^5 years from records in Turkmenia, which is exceptionally long. Except for the anomalous value from Turkmenia, the other results are consistent with the duration of a typical polarity transition.

[29] The relative paleointensity started to decrease at 20 kyr before the G-M transition (Figures 8 and 11). In contrast, it reached a local peak in less than

10 kyr after the end of transition. This asymmetric behavior, gradual decay preceding the transition and rapid recovery after the transition, is consistent with those of polarity transitions occurred during the past 2 Myrs pointed out by *Valet et al.* [2005]. However, the duration of decay preceding the transition in the present result is much shorter than the 60–80-kyr-long decay described by *Valet et al.* [2005]; the present result has a clear peak 20 kyr before the transition, with a gradually decay in the intensity afterwards. The duration of decay preceding the G-M transition is ~ 80 kyr in the EPAPIS-3Ma record [*Yamazaki and Oda*, 2005], ~ 60 kyr in the OJP-stack record [*Kok and Tauxe*, 1999], and ~ 40 kyr in the record of ODP Leg 138 [*Valet and Meynadier*, 1993], respectively. The values diverge widely and it is difficult to draw a conclusion from the fairly limited number of transitional records whether the duration of decay preceding the G-M transition is different from those of polarity transitions that have occurred during the past 2 Myrs.

[30] A characteristic of the temporal variation in the latitude of VGP in Figure 11 is its north-south-north-south rebounding. A detailed description and discussion of the VGP path of U1314 record at G-M transition is given in *Ohno et al.* [2008]. Here we note that the period for rebounding of VGP is ~ 4 kyr for the first north-south-north rebounding and ~ 2 kyr for the latter south-north-south rebounding; it is interesting to note that they are similar value to the duration of geomagnetic excursions.

5. Conclusions

[31] Temporal variation in the geomagnetic field between 2.1 and 2.75 Ma was studied from a sediment core in the Gardar drift, north Atlantic. Well defined characteristic directional records and relative paleointensity record were obtained. The paleointensity lows correspond well with those in paleointensity record in the Pacific (EPAPIS-3Ma and OJP-stack). Since the sedimentation rate of this core is much higher than that of the previously studied records, details of the geomagnetic field in this period were revealed that had not been previously observed.

[32] First, eight paleointensity lows were observed in addition to the lows at the Gauss-Matuyama (G-M) transition and the Réunion Subchron. These paleointensity lows are associated with large directional changes (geomagnetic excursions). Among the eight geomagnetic excursions, the older five

excursions are found in the period in which no geomagnetic excursions have ever been reported from marine sediments. The high fidelity of the U1314 paleomagnetic record and its ability to resolve excursions is attributed to the higher sedimentation rate at Site U1314 relative to previously studied sedimentary sections in this period.

[33] Second, we determined that G-M transition had duration of 5,000 years and that it occurred within MIS 103, even if we consider an error in depth of up to 20 cm due to delayed lock-in of magnetic particles. During the G-M transition and the top and the bottom Réunion transitions, the paleointensity was <20% of the average value of the whole interval studied. Asymmetric behavior of paleointensity was observed associated with the G-M transition; the paleointensity started to decrease 20 kyr before the transition, and recovered in less than 10 kyr after the transition.

Appendix A: New Age Model for EPAPIS-3Ma

[34] In Figure 10, we compare the paleointensity lows between 2.25 and 2.75 Ma in U1314 and EPAPIS-3Ma [Yamazaki and Oda, 2005]. The age model of EPAPIS-3Ma is based on MD982187 for 2.16–3 Ma, which was dated by matching of ARM and/or magnetic susceptibility with oxygen isotope curve from ODP Site 1143 [Tian et al., 2002]. Ao et al. [2011] has published a new age model for Site 1143 by tuning their environmental proxy to LR04 record and the 65°N summer insolation. The difference in the age of the paleointensity lows in the EPAPIS-3Ma record between the old and new age models is negligible except for the paleointensity low in EPAPIS-3Ma at 2.57 Ma (corresponding to L4 in U1314); it shifts the age of the paleointensity low to an age 16 kyr older. Regardless of which age model is used, the paleointensity lows in EPAPIS-3Ma are older on average than those in U1314 by ca. 20 kyr.

Acknowledgments

[35] This study used samples provided by the Integrated Ocean Drilling Program (IODP). We are indebted to the staff of the RV JOIDES Resolution and the IODP Bremen Core Repository for their support. This study was performed under the cooperative research program of Center for Advanced Marine Core Research (CMCR), Kochi University (09A010 and 09B010). This study was partly supported by JSPS Grant-in-Aid for Scientific Research (22241006). We would like to thank A. Mazaud and A. Grinsted for providing computer programs, and T. Yamazaki and Y. S. Kok-Palma for providing

paleointensity data (EPAPIS-3Ma and OJP-stack, respectively). We acknowledge comments given by anonymous reviewers and the associated editor that substantially improved this manuscript.

References

- Ao, H., M. J. Dekkers, L. Qin, and G. Xiao (2011), An updated astronomical timescale for the Plio-Pleistocene deposits from South China Sea and new insights into Asian monsoon evolution, *Quat. Sci. Rev.*, *30*, 1560–1575, doi:10.1016/j.quascirev.2011.04.009.
- Burakov, K. S., G. Z. Gurary, A. N. Khramov, G. N. Petrova, G. V. Rassanova, and V. P. Rodinov (1976), Some peculiarities of the virtual pole positions during reversals, *J. Geomagn. Geoelectr.*, *28*, 295–307, doi:10.5636/jgg.28.295.
- Cande, S. C., and D. V. Kent (1995), Revised calibration of the geomagnetic polarity timescale for the Late Cretaceous and Cenozoic, *J. Geophys. Res.*, *100*(B4), 6093–6095, doi:10.1029/94JB03098.
- Channell, J. E. T. (1999), Geomagnetic paleointensity and directional secular variation at Ocean Drilling Program (ODP) Site 984(Bjorn Drift) since 500 ka: Comparisons with ODP Site 983(Gardar Drift), *J. Geophys. Res.*, *104*, 22,937–22,951, doi:10.1029/1999JB900223.
- Channell, J. E. T. (2006), Late Brunhes polarity excursions (Mono Lake, Laschamp, Iceland Basin and Pringle Falls) recorded at ODP Site 919(Irminger Basin), *Earth Planet. Sci. Lett.*, *244*, 378–393, doi:10.1016/j.epsl.2006.01.021.
- Channell, J. E. T., and Y. Guyodo (2004), The Matuyama Chronozone at ODP Site 982 (Rockall Bank): Evidence for decimeter-scale magnetization lock-in depth, in *Time-scales of the Paleomagnetic Field*, *Geophys. Monogr. Ser.*, vol. 145, edited by J. E. T. Channell et al., pp. 205–219, AGU, Washington, D. C., doi:10.1029/145GM15.
- Channell, J. E. T., and H. F. Kleiven (2000), Geomagnetic paleointensities and astronomical ages for the Matuyama-Brunhes boundary and the boundaries of the Jaramillo Subchron: Paleomagnetic and oxygen isotope records from ODP Site 983, *Philos. Trans. R. Soc. London, Ser. A*, *358*, 1027–1047, doi:10.1098/rsta.2000.0572.
- Channell, J. E. T., and M. E. Raymo (2003), Paleomagnetic record at ODP Site 980 (Feni Drift, Rockall) for the past 1.2 Myrs, *Geochem. Geophys. Geosyst.*, *4*(4), 1033, doi:10.1029/2002GC000440.
- Channell, J. E. T., D. A. Hodell, and B. Lehman (1997), Relative geomagnetic paleointensity and δO^{18} at ODP Site 983 (Gardar Drift, North Atlantic) since 350 ka, *Earth Planet. Sci. Lett.*, *153*, 103–118, doi:10.1016/S0012-821X(97)00164-7.
- Channell, J. E. T., A. Mazaud, P. Sullivan, S. Turner, and M. E. Raymo (2002), Geomagnetic excursions and paleointensities in the Matuyama Chron at Ocean Drilling Program Sites 983 and 984 (Iceland Basin), *J. Geophys. Res.*, *107*(B6), 2114, doi:10.1029/2001JB000491.
- Channell, J. E. T., L. Labs, and M. E. Raymo (2003), The Réunion Subchronozone at ODP Site 981 (Feni Drift, North Atlantic), *Earth Planet. Sci. Lett.*, *215*, 1–12, doi:10.1016/S0012-821X(03)00435-7.
- Channell, J. E. T., J. H. Curtis, and B. P. Flower (2004), The Matuyama-Brunhes boundary interval (500–900 ka) in North Atlantic drift sediments, *Geophys. J. Int.*, *158*, 489–505, doi:10.1111/j.1365-246X.2004.02329.x.
- Channell, J. E. T., D. A. Hodell, C. Xuan, A. Mazaud, and J. S. Stoner (2008), Age calibrated relative paleointensity for the last

- 1.5 Myr at IODP Site U1308 (North Atlantic), *Earth Planet. Sci. Lett.*, *274*, 59–71, doi:10.1016/j.epsl.2008.07.005.
- Channell, J. E. T., C. Xuan, and D. A. Hodell (2009), Stacking paleointensity and oxygen isotope data for the last 1.5 Myr (PISO-1500), *Earth Planet. Sci. Lett.*, *283*, 14–23, doi:10.1016/j.epsl.2009.03.012.
- Channell, J. E. T., D. A. Hodell, B. S. Singer, and C. Xuan (2010), Reconciling astrochronological and $^{40}\text{Ar}/^{39}\text{Ar}$ ages for the Matuyama-Brunhes boundary and late Matuyama Chron, *Geochem. Geophys. Geosyst.*, *11*, Q0AA12, doi:10.1029/2010GC003203.
- Clement, B. M. (2004), Dependence of the duration of geomagnetic polarity reversals on site latitude, *Nature*, *428*, 637–640, doi:10.1038/nature02459.
- Day, R., M. Fuller, and V. A. Schmidt (1977), Hysteresis properties of titanomagnetites: Grain-size and compositional dependence, *Phys. Earth Planet. Inter.*, *13*, 260–267, doi:10.1016/0031-9201(77)90108-X.
- Deino, A., J. Kingston, J. Glen, R. Edgar, and A. Hill (2006), Precessional forcing of lacustrine sedimentation in the late Cenozoic Chemeron Basin, Central Kenya Rift, and calibration of the Gauss/Matuyama boundary, *Earth Planet. Sci. Lett.*, *247*, 41–60.
- Dreyfus, G. B., G. M. Raisbeck, F. Parrenin, J. Jouzel, Y. Guyodo, S. Nomade, and A. Mazaud (2008), An ice core perspective on the age of the Matuyama-Brunhes boundary, *Earth Planet. Sci. Lett.*, *274*, 151–156, doi:10.1016/j.epsl.2008.07.008.
- Dunlop, D. J. (2002a), Theory and application of the Day plot (M_{rs}/M_s versus H_{cr}/H_c): 1. Theoretical curves and tests using titanomagnetite data, *J. Geophys. Res.*, *107*(B3), 2056, doi:10.1029/2001JB000486.
- Dunlop, D. J. (2002b), Theory and application of the Day plot (M_{rs}/M_s versus H_{cr}/H_c): 2. Application to data for rocks, sediments, and soils, *J. Geophys. Res.*, *107*(B3), 2057, doi:10.1029/2001JB000487.
- Expedition 306 Scientists (2006), Site U1314, *Proc. Integrated Ocean Drill. Program*, *306*, 1–95.
- Glen, J. M. G., R. S. Coe, and J. C. Liddicoat (1999), A detailed record of paleomagnetic field change from Searles Lake, California: 2. The Gauss/Matuyama polarity reversal, *J. Geophys. Res.*, *104*, 12,883–12,894, doi:10.1029/1999JB900048.
- Grinsted, A., J. C. Moore, and S. Jevrejeva (2004), Application of the cross wavelet transform and wavelet coherence to geophysical time series, *Nonlinear Processes Geophys.*, *11*, 561–566, doi:10.5194/npg-11-561-2004.
- Guyodo, Y., and J. E. T. Channell (2002), Effects of variable sedimentation rates and age errors on the resolution of sedimentary paleointensity records, *Geochem. Geophys. Geosyst.*, *3*(8), 1048, doi:10.1029/2001GC000211.
- Guyodo, Y., and J. P. Valet (1999a), Integration of volcanic and sedimentary records of paleointensity: Constraints imposed by irregular eruption rates, *Geophys. Res. Lett.*, *26*, 3669–3672, doi:10.1029/1999GL008422.
- Guyodo, Y., and J.-P. Valet (1999b), Global changes in intensity of the Earth's magnetic field during the past 800 kyr, *Nature*, *399*, 249–252, doi:10.1038/20420.
- Guyodo, Y., P. Gaillot, and J. E. T. Channell (2000), Wavelet analysis of relative geomagnetic paleointensity at ODP Site 983, *Earth Planet. Sci. Lett.*, *184*, 109–123, doi:10.1016/S0012-821X(00)00313-7.
- Hayashi, T., M. Ohno, G. Acton, Y. Guyodo, H. F. Evans, T. Kanamatsu, F. Komatsu, and F. Murakami (2010), Millennial-scale iceberg surges after intensification of Northern Hemisphere glaciation, *Geochem. Geophys. Geosyst.*, *11*, Q09Z20, doi:10.1029/2010GC003132.
- Kirschvink, J. L. (1980), The least-squares lines and plane and analysis of paleomagnetic data, *Geophys. J. R. Astron. Soc.*, *62*, 699–718, doi:10.1111/j.1365-246X.1980.tb02601.x.
- Kok, Y. S., and L. Tauxe (1999), A relative geomagnetic paleointensity stack from Ontong-Java Plateau sediments for the Matuyama, *J. Geophys. Res.*, *104*, 25,401–25,413, doi:10.1029/1999JB900186.
- Kuiper, K. F., F. J. Hilgen, J. Steenbrink, and J. R. Wijbrans (2004), $^{40}\text{Ar}/^{39}\text{Ar}$ ages of tephrae intercalated in astronomically tuned Neogene sedimentary sequences in the eastern Mediterranean, *Earth Planet. Sci. Lett.*, *222*, 583–597.
- Laj, C., and J. E. T. Channell (2007), Geomagnetic excursions, in *Treatise on Geophysics*, vol. 5, *Geomagnetism*, edited by M. Kono, pp. 373–416, Elsevier, Amsterdam, doi:10.1016/B978-044452748-6.00095-X.
- Lisiecki, L. E., and M. E. Raymo (2005), A Pliocene-Pleistocene stack of 57 globally distributed benthic $\delta^{18}\text{O}$ records, *Paleoceanography*, *20*, PA1003, doi:10.1029/2004PA001071.
- Liu, Q. S., A. P. Roberts, E. J. Rohling, R. X. Zhu, and Y. B. Sun (2008), Post-depositional remanent magnetization lock-in and the location of the Matuyama-Brunhes geomagnetic reversal boundary in marine and Chinese loess sequences, *Earth Planet. Sci. Lett.*, *275*, 102–110, doi:10.1016/j.epsl.2008.08.004.
- Lourens, L. J., A. Antonarakou, F. J. Hilgen, A. A. M. Van Hoof, C. Vergnaud-Grazzini, and W. J. Zachariasse (1996), Evaluation of the Plio-Pleistocene astronomical timescale, *Paleoceanography*, *11*, 391–413, doi:10.1029/96PA01125.
- Lourens, L., F. J. Hilgen, N. J. Shackleton, J. Laskar, and D. Wilson (2004), The Neogene period, in *A Geologic Time Scale 2004*, edited by F. M. Gradstein, J. G. Ogg, and A. G. Smith, pp. 409–440, Cambridge Univ. Press, Cambridge, U. K.
- Lund, S., J. S. Stoner, J. E. T. Channell, and G. Acton (2006), A summary of Brunhes paleomagnetic field variability recorded in Ocean Drilling Program cores, *Phys. Earth Planet. Inter.*, *156*, 194–204, doi:10.1016/j.pepi.2005.10.009.
- Mazaud, A. (2005), User-friendly software for vector analysis of the magnetization of long sediment cores, *Geochem. Geophys. Geosyst.*, *6*, Q12006, doi:10.1029/2005GC001036.
- Merrill, R. T., and P. L. McFadden (1999), Geomagnetic polarity transition, *Rev. Geophys.*, *37*, 201–226, doi:10.1029/1998RG900004.
- Oda, H. (2005), Recurrent geomagnetic excursions: A review for the Brunhes normal polarity chron [in Japanese with English abstract], *J. Geogr.*, *114*, 174–193, doi:10.5026/jgeography.114.2_174.
- Ohno, M., F. Murakami, F. Komatsu, Y. Guyodo, G. Acton, T. Kanamatsu, H. F. Evans, and F. Nanayama (2008), Paleomagnetic directions of the Gauss-Matuyama polarity transition recorded in drift sediments (IODP Site U1314) in the North Atlantic, *Earth Planets Space*, *60*, e13–e16.
- Roberts, A. P., and M. Winklhofer (2004), Why are geomagnetic excursions not always recorded in sediments? Constraints from post-depositional remanent magnetization lock-in modeling, *Earth Planet. Sci. Lett.*, *227*, 345–359, doi:10.1016/j.epsl.2004.07.040.
- Suganuma, Y., Y. Yokoyama, T. Yamazaki, K. Kawamura, C.-S. Horng, and H. Matsuzaki (2010), ^{10}Be evidence for delayed acquisition of remanent magnetization in marine sediments: Implication for a new age for the Matuyama–



- Brunhes boundary, *Earth Planet. Sci. Lett.*, *296*, 443–450, doi:10.1016/j.epsl.2010.05.031.
- Tauxe, L. (1993), Sedimentary records of relative paleointensity of the geomagnetic field: Theory and practice, *Rev. Geophys.*, *31*, 319–354, doi:10.1029/93RG01771.
- Tauxe, L., and T. Yamazaki (2007), Paleointensities, in *Treatise on Geophysics*, vol. 5, *Geomagnetism*, edited by M. Kono, pp. 509–563, Elsevier, Amsterdam, doi:10.1016/B978-044452748-6.00098-5.
- Tian, J., P. Wang, X. Cheng, and Q. Li (2002), Astronomically tuned Plio-Pleistocene benthic $\delta^{18}\text{O}$ record from South China Sea and Atlantic-Pacific comparison, *Earth Planet. Sci. Lett.*, *203*, 1015–1029, doi:10.1016/S0012-821X(02)00923-8.
- Valet, J.-P., and L. Meynadier (1993), Geomagnetic field intensity and reversals during the past four million years, *Nature*, *366*, 234–238, doi:10.1038/366234a0.
- Valet, J.-P., L. Meynadier, and Y. Guyodo (2005), Geomagnetic dipole strength and reversal rate over the past two million years, *Nature*, *435*, 802–805, doi:10.1038/nature03674.
- Yamamoto, Y., O. Ishizuka, M. Sudo, and K. Uto (2007a), $^{40}\text{Ar}/^{39}\text{Ar}$ ages and palaeomagnetism of transitionally magnetized volcanic rocks in the Society Islands, French Polynesia: Raiatea excursion in the upper-Gauss Chron, *Geophys. J. Int.*, *169*, 41–59, doi:10.1111/j.1365-246X.2006.03277.x.
- Yamamoto, Y., T. Yamazaki, T. Kanamatsu, N. Ioka, and T. Mishima (2007b), Relative paleointensity stack during the last 250 kyr in the northwest Pacific, *J. Geophys. Res.*, *112*, B01104, doi:10.1029/2006JB004477.
- Yamazaki, T. (2008), Magnetostatic interactions in deep-sea sediments inferred from first-order reversal curve diagrams: Implications for relative paleointensity normalization, *Geochem. Geophys. Geosyst.*, *9*, Q02005, doi:10.1029/2007GC001797.
- Yamazaki, T., and H. Oda (2005), A geomagnetic paleointensity stack between 0.8 and 3.0 Ma from equatorial Pacific sediment cores, *Geochem. Geophys. Geosyst.*, *6*, Q11H20, doi:10.1029/2005GC001001.
- Yang, T. S., M. Hyodo, Z. Y. Yang, L. Ding, J. L. Fu, and T. Mishima (2007), Early and middle Matuyama geomagnetic excursions recorded in the Chinese loess-paleosol sediments, *Earth Planets Space*, *59*, 825–840.
- Zhao, M., M. Ohno, Y. Kuwahara, T. Hayashi, and T. Yamashita (2011), Magnetic minerals in sediments from IODP Site U1314 determined by low-temperature and high-temperature magnetism, *Bull. Grad. Sch. Soc. Cult. Stud. Kyushu Univ.*, *17*, 77–84.
- Zhu, R. X., B. Guo, Z. L. Ding, Z. T. Guo, A. Kazansky, and G. Matasova (2000), Gauss-Matuyama polarity transition obtained from a loess section at Weinan, north-central China, *Chin. J. Geophys.*, *43*, 654–671.